

Hole Growth as a Microrheological Probe to Measure the Viscosity of Polymers Confined to Thin Films

CONNIE B. ROTH,* JOHN R. DUTCHER

Department of Physics and the Guelph-Waterloo Physics Institute, University of Guelph, Guelph, Ontario N1G 2W1, Canada

Received 30 December 2005; accepted 28 March 2006

DOI: 10.1002/polb.20918

Published online in Wiley InterScience (www.interscience.wiley.com).

ABSTRACT: We review recent hole growth measurements performed at elevated temperatures in freely-standing polystyrene (PS) films, using optical microscopy and a differential pressure experiment (DPE). In the hole growth experiments, which were performed at temperatures close to the bulk glass-transition temperature of PS, $T_g^{\text{bulk}} = 97^\circ\text{C}$, we find evidence for nonlinear viscoelastic effects, which markedly affect the growth of holes in freely-standing PS films. The hole radius R initially grew linearly with time t before undergoing a transition to exponential growth characterized by a growth time τ . The time scale τ_1 for the decay of the initial transient behavior prior to reaching steady state was consistent with the convective constraint release mechanism of the tube theory of entangled polymer dynamics, while the characteristic hole growth times τ of the holes were consistent with significant reductions in viscosity of over eight orders of magnitude with increasing shear strain rate due to shear thinning. DPE measurements of hole growth on very thin freely-standing films revealed that hole formation and growth occurs only at temperatures that are comparable to or greater than T_g^{bulk} , even for films for which the T_g value was reduced by many tens of degrees Celsius below the bulk value. © 2006 Wiley Periodicals, Inc. *J Polym Sci Part B: Polym Phys* 44: 3011–3021, 2006

Keywords: glass transition; nanoscale confinement; rheology; thin films; viscoelastic properties

INTRODUCTION

The dynamics of polymers confined to thin films have been studied extensively showing reductions in the glass-transition temperature T_g with decreasing film thickness h for both supported and freely-standing films (see for instance refs. 1–15 and references therein). The most significant T_g reductions observed to date are for high molecular weight M_w freely-standing polystyrene (PS) films, for which T_g values reduced by as much as 80°C

from the bulk value have been measured for films of thickness $h = 36\text{ nm}$ of $M_w = 1.25 \times 10^6$.^{3,4,7} Measurements of the dynamics in thin films at longer length scales are less conclusive with several diffusion studies suggesting that mobility on the length scale of the entire chain is not enhanced substantially,^{16–19} or even reduced,^{20–25} relative to that in the bulk. The formation and growth of holes at elevated temperatures has also been used as a probe of chain dynamics in thin polymer films both in supported films,^{26–35} and in freely-standing films.^{36–43} The key difference between the chain diffusion and hole growth studies in thin polymer films is that hole growth is a driven process due to surface tension acting at the edge of the hole, which results in high shear strain rates and corresponding nonlinear viscoelastic behavior.

*Present address: Department of Chemical and Biological Engineering, Northwestern University, Evanston, Illinois 60208-3120.

Correspondence to: J. R. Dutcher (E-mail: dutcher@physics.uoguelph.ca)

Journal of Polymer Science: Part B: Polymer Physics, Vol. 44, 3011–3021 (2006)
© 2006 Wiley Periodicals, Inc.

The freely-standing film geometry is appealing because the in-plane component of the fluid velocity is uniform across the thickness of the film, corresponding to plug flow, since the film is symmetric with respect to the mid-plane of the film. For holes growing in freely-standing liquid films of low viscosity, e.g. soap films,^{44–46} the time rate of change of the surface energy due to surface tension is balanced by the time rate of change of the kinetic energy due to inertia, which leads to linear growth of the hole radius with time. In freely-standing liquid films with large viscosity, hole growth is determined by the balance between surface energy and viscous damping, which leads to exponential growth of the hole radius with time.^{36–38,41,44}

$$R(t) = R_0 \exp(t/\tau), \quad (1)$$

where τ is the characteristic growth time of the holes. The values of τ measured in hole growth experiments can be used to obtain two quantities: the film viscosity η at the edge of the hole,

$$\eta = \frac{\epsilon\tau}{h}, \quad (2)$$

where h is the film thickness and ϵ is the surface tension; and the shear strain rate $\dot{\gamma}$ at the edge of the hole,³⁸

$$\dot{\gamma} = \frac{2\dot{R}}{R} = \frac{2}{\tau}. \quad (3)$$

Thus, hole growth provides a rheological probe of nanoscopically-confined chain dynamics over micrometer in-plane distances in thin polymer films with $R(t)$ representing the deformation (strain) of the material as a result of the constant applied stress

$$\sigma = \frac{2\epsilon}{h} \quad (4)$$

acting radially outward at the edge of the hole. For small film thicknesses h , the stress σ can be substantial: for $h = 50$ nm, eq 4 gives a stress of 1.2 MPa, increasing as $1/h$ as the film thickness is decreased. For holes growing in freely-standing viscous films, a rim of liquid does not form at the edge of the hole, as confirmed by atomic force microscopy (AFM) measurements,^{41,43} instead the film thickens uniformly.^{36–38,41,44}

In this article, we present a summary of results obtained from hole growth measurements performed on thin freely-standing PS films using

both optical microscopy and a differential pressure experiment (DPE). We have focused our hole growth measurements on thin PS films because very large reductions in T_g are observed for these films for very small film thicknesses. In the optical microscopy studies, we find that the hole radius $R(t)$ exhibits an unusual transition from linear to exponential growth as hole growth proceeds at temperatures that are comparable to the bulk value of the glass-transition temperature T_g^{bulk} . This transient linear growth behavior, prior to reaching the steady-state exponential growth behavior, is consistent with the decay of entanglements via the convective constraint release (CCR) mechanism of the tube theory for entangled polymer dynamics. The values of the apparent viscosity η at the edge of the hole during steady state, determined from the values of the characteristic growth times τ measured during the late stages of hole growth, are decreased by up to eight orders of magnitude with increasing strain rate in agreement with the bulk phenomenon of shear thinning. Using the DPE, we have found that the onset of hole formation and growth occurs at temperatures that are comparable to $T_g^{\text{bulk}} = 97^\circ\text{C}$, and are only several degrees below T_g^{bulk} for very thin films with T_g reductions of many tens of degrees. The small differences between the τ values obtained for thicker and thinner films are quantitatively consistent with shear thinning as a result of the increased stress σ present at the edge of the growing hole in the thinner films (see eq 4). We finish by discussing the disparity between mobility at different length scales in thin polymer films.

EXPERIMENTS

The PS films were spincoated onto freshly-cleaved mica substrates using dilute solutions of narrow distribution PS, with molecular weights ranging from 120×10^3 to 2240×10^3 ($M_w/M_n < 1.12$), dissolved in toluene (0.9 to 2.3% PS by mass) and at an angular speed of 4000 rpm. The PS films on the mica substrates were annealed under vacuum for 12 h at 115°C to remove trapped solvent molecules, and then cooled slowly ($\leq 1^\circ\text{C}/\text{min}$) to room temperature to produce a well-defined and reproducible thermal history. Freely-standing PS films were made using a water transfer technique⁴ to remove the PS film from the mica substrate and place a piece of the PS film across a 4-mm diameter hole in a stainless steel sample holder.

Freely-standing PS films were heated to the measurement temperature T , either in a hot stage on the optical microscope or in the differential pressure experiment (DPE) cell. The temperature was increased quickly to the measurement temperature, and holes were observed to form spontaneously in the films because of nucleation at dust or defect sites. Precise measurements of the radius R of a single growing hole as a function of time t were obtained using optical microscopy by capturing a time series of optical images.⁴¹ The characteristic growth time τ was also determined using the DPE by measuring the rate of gas flow through many small holes, which form at elevated temperatures over the 4-mm diameter of the freely-standing PS film.^{39,40} In the DPE, a small pressure difference ($<10^{-4}$ atm) is maintained across the freely-standing film by actively controlling the position of a piston which adjusts the gas pressure on one side of the film. The measured position of the piston as a function of time is fit to a functional form to extract the growth time τ , as well as the mean time t_0 for hole formation to occur.³⁹ The DPE is more suitable than optical microscopy for measuring hole growth in very thin films at the lowest measurement temperatures because of the difficulty in visually identifying slowly growing holes in the optical microscope at very low temperatures.

RESULTS

Optical Microscopy: Growth of a Single Hole

Optical microscopy measurements⁴¹ of the hole radius $R(t)$ in freely-standing polystyrene films at temperatures very close to T_g^{bulk} revealed a transition from an initial linear dependence of R on t to an exponential dependence of R on t . The exponential dependence of R on t has been observed previously for freely-standing viscous films^{36–38} and can be understood theoretically from the balance of the time rate of change of the viscous and surface energies (see Introduction). The initial linear dependence of R on t was unexpected. This complex dependence of R on t is illustrated in Figure 1 by plotting a typical $R(t)$ data set in two different ways: (a) the R values plotted on a linear axis versus time t , which shows linear hole growth at early times, and (b) the R values plotted on a natural logarithmic axis versus time t , which shows that exponential growth is obtained during the late stages of hole growth. We have observed the transition from linear to

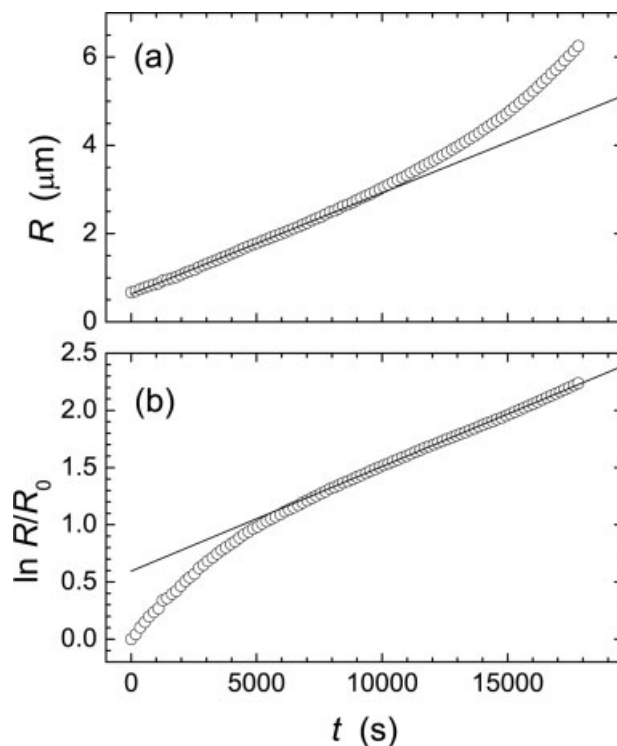


Figure 1. Hole radius $R(t)$ data for a freely-standing PS film of $M_w = 2240 \times 10^3$ and $h = 79$ nm held at $T = 103^\circ\text{C}$ with (a) linear and (b) natural logarithmic axes for the R values. The straight solid lines in the plots correspond to best fits to (a) $R(t) = vt + c$, with $v = 0.23$ nm/s and $c = 0.63$ μm , for $0 < t < 7740$ s; and (b) $R(t) = Ae^{t/\tau}$, with $\tau = 10900$ s and $A = 1.21$ μm , for 8100 s $< t < 17820$ s.

exponential hole growth for films with different molecular weights ($M_w = 282 \times 10^3$, 717×10^3 , and 2240×10^3), different thicknesses ($h = 61$ – 125 nm), and at temperatures T within the range $101^\circ\text{C} < T < 117^\circ\text{C}$. The initial linear regime is most apparent in the data sets for films with larger molecular weights measured at the lowest temperatures.

All of the measured $R(t)$ data were found to be well fit by an empirical equation:⁴¹

$$R(t) = R_0 \exp\left(\frac{t}{\tau} \left[1 + \exp\left(-\frac{t}{\tau_1}\right)\right]\right). \quad (5)$$

This functional form can be interpreted as exponential growth of $R(t)$ in a viscous material with a time varying viscosity $\eta(t)$ that increases to a steady-state value η_∞ as

$$\eta(t) = \frac{\eta_\infty}{1 + \exp\left(-\frac{t}{\tau_1}\right)}. \quad (6)$$

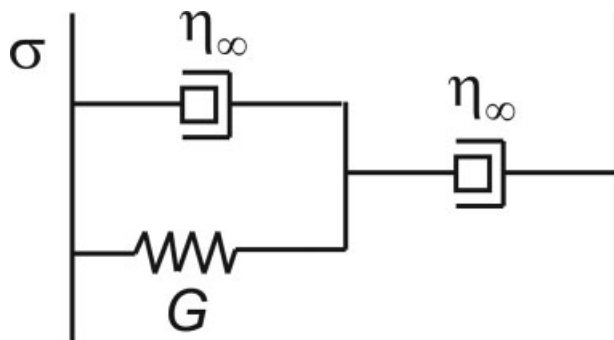


Figure 2. A spring and dashpot model corresponding to a viscoelastic fluid describing the time-dependent strain $\gamma(t)$ given by eq 7: the dashpots have a viscosity η_∞ and the spring has a modulus G .

Interestingly, this functional form for $\eta(t)$ is equivalent to a three parameter spring and dashpot model for a simple viscoelastic fluid, shown in Figure 2. We can think of hole growth as the time-dependent deformation (pure shear strain) of the polymer chains in response to the constant applied stress, $\sigma = 2\epsilon/h$, because of surface tension acting at the edge of the hole.⁴⁷ The spring and dashpot model shown in Figure 2 describes the time-dependent strain response of the system because of a constant applied stress σ .⁴¹

$$\gamma(t) = \sigma \left(\frac{t}{\eta_\infty} + \frac{1}{G} \left[1 + \exp\left(-\frac{G}{\eta_\infty} t\right) \right] \right). \quad (7)$$

In Figure 2, the dashpots have a viscosity η_∞ corresponding to the viscosity value during the late stages of hole growth, which is reduced from the zero shear strain rate value η_0 due to shear thinning, and the spring has a shear modulus G . Equation 7 corresponds to the time-dependent viscosity $\eta(t) = \sigma/\dot{\gamma}$ given by eq 6, where $\tau_1 = \eta_\infty/G$ is the time constant for the decay of transient effects in the system.

For the steady-state behavior observed at long times, we use the characteristic growth of $R(t)$ in this regime to determine an apparent viscosity of the film $\eta_\infty (\equiv \eta)$ near the edge of the hole via eq 2. The derivation of exponential growth of the hole radius, eq 1, with a characteristic growth time τ related to the material properties of the film by eq 2, is based on a balance between the time rate of change of the surface energy due to surface tension,

$$\dot{E}_{\text{surf}}(r) = (2\epsilon)2\pi R\dot{R}, \quad (8)$$

and viscous dissipation,

$$\dot{E}_{\text{kin}}(r) = 2 \int_R^\infty 2\pi r h \eta dr \left[\left(\frac{\partial v}{\partial r} \right)^2 + \left(\frac{v}{r} \right)^2 \right]. \quad (9)$$

For a simple viscous fluid, the viscosity is independent of the radial distance r and eqs 1 and 2 are easily recovered. However, for the present case, as we will show, the viscosity at the edge of the hole is reduced from that in the rest of the film because of shear thinning. A radial dependence of viscosity $\eta(r)$ is expected with softer material at the edge of the hole and with $\eta(r)$ gradually increasing until η_0 is recovered sufficiently far away from the hole. As such, the use of eq 2 is technically not valid. Nonetheless, we argue that for sufficiently thick films, for which the stress at the edge of the hole is less, and at sufficiently high temperatures and long times polystyrene will behave as a viscous fluid, eq 2 will be valid and exponential growth will be observed. We only observe deviations in $R(t)$ from exponential growth for temperatures $T \lesssim 117^\circ\text{C}$ for film thicknesses on the order of a hundred nanometers. These deviations in $R(t)$ occur as an initial transient behavior at short times before the steady-state exponential growth behavior is recovered at long times. We feel that use of eq 2 is valid in the steady-state regime when exponential growth is observed allowing us to characterize the observed flow by an effective viscosity.

The apparent viscosity values η that we calculate from the values of τ in the steady-state regime according to eq 2 represent the viscosity of the material in the region near the edge of the hole. These viscosity values are plotted in Figure 3 as a function of the reduced shear strain rate β , where the viscosity values have been normalized to the zero shear strain rate η_0 values determined for the different M_w and T values used in the hole growth experiments from viscosity values measured for bulk polystyrene.^{40,48,49} The use of the reduced shear strain rate β ⁵⁰

$$\beta = \frac{\eta_0 M_w \dot{\gamma}}{\rho R_{\text{mol}} T}, \quad (10)$$

where ρ is the density of the polymer and R_{mol} is the molar gas constant, allows the viscosity values measured for films with different values of h , M_w , and T to be plotted on the same graph. The data presented in Figure 3 is compiled from τ values measured using optical microscopy from three separate studies^{38,41,42} and from the differential pressure experiment (described in the next

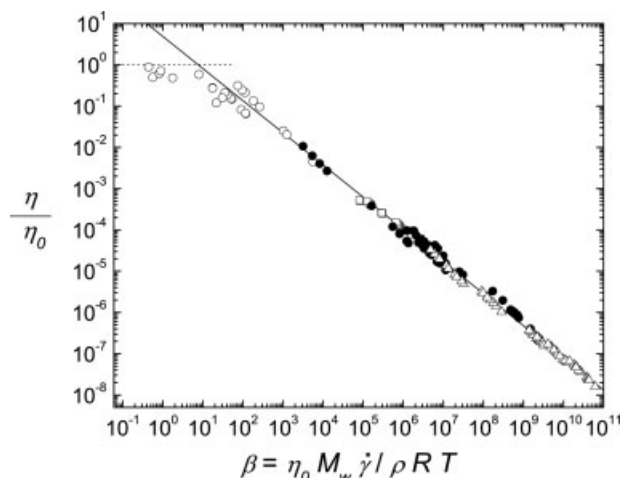


Figure 3. Viscosity η at the edge of the hole determined from hole growth measurements of freely-standing PS films at temperatures close to and above T_g^{bulk} , divided by the zero shear rate viscosity η_0 , as a function of the reduced shear strain rate $\beta = \eta_0 M_w \dot{\gamma} / \rho R T$ for studies of hole growth in freely-standing PS films using optical microscopy (data from ref. 41 (●), ref. 38 (□) and ref. 42 (○)) and the DPE (Δ) (data from ref. 39 and 40). The slope of the best fit line through all of the (● and Δ) data is -0.78 ± 0.01 .

section), which extends the data to lower temperatures and therefore larger values of β .^{39,40} The most striking feature of Figure 3 is the power law decrease that is observed in the viscosity values over eight orders of magnitude with increasing reduced shear strain rate β that spans twelve orders of magnitude. The slope of the $\log_{10}(\eta/\eta_0)$ vs. $\log_{10} \beta$ data in Figure 3 is -0.78 ± 0.01 ^{40,41} which is consistent with the value of ~ -0.8 that is measured in bulk rheology experiments by varying the shear strain rate value by two orders of magnitude.^{50,51}

The early stage dynamics of hole growth are characterized by a second time constant τ_1 (cf. eq 5), which describes the exponential decay of the transient behavior to the simple exponential increase of $R(t)$ that is observed at long times. As holes form and grow in the freely-standing PS films, the entanglement between chains decreases from an initially high value corresponding to the annealed, spincoated film to a much lower value corresponding to the highly sheared state with markedly reduced values of the viscosity.

The shear modulus G associated with the spring in the simple viscoelastic model shown in Figure 2 can be calculated from the equation $G = \eta_\infty / \tau_1$ using the best fit values of η_∞ and τ_1 obtained from the measured $R(t)$ data. The shear modulus

G describes the stiffness of the PS during the early stages of hole growth, according to eq 7, and its value is a measure of the initial entanglement density relative to that in bulk. The values calculated for G range from 4×10^5 Pa to 1.5×10^6 Pa showing no systematic variation with M_w , T , or h . The average value of $G \approx 9.5 \times 10^5$ Pa is in reasonable agreement with literature values for the plateau shear modulus of bulk polystyrene ($\sim 2 \times 10^5$ Pa).^{52,53} The values of the shear modulus G obtained from the present study can be compared with the anomalously high values of the plateau modulus that were inferred from membrane deflection experiments of freely-standing poly(vinyl acetate) (PVAc) films,⁵⁴ and measurements of the extension ratio in uniaxially strained freely-standing glassy PS films that suggest that the density of entanglements (and therefore the plateau modulus) in thin films is less than that of bulk samples.⁵⁵

It is perhaps surprising that the holes in freely-standing PS films form and grow over time scales that are shorter than the reptation time of the polymer at low measurement temperatures that are close to T_g^{bulk} . At a temperature of 101°C , the reptation time τ_d varies from 4×10^5 to 8×10^9 s for the range of molecular weights used,⁴⁷ yet hole growth occurs over a shorter time scale ($\sim 10^4$ s). According to the tube theory for entangled polymer dynamics, reptation is the dominant relaxation mechanism only for linear monodisperse chains at small shear strain rates ($\dot{\gamma} < \tau_d^{-1}$).⁵⁶⁻⁵⁹ For intermediate shear rates greater than τ_d^{-1} yet less than τ_R^{-1} , where τ_R is the time of the longest Rouse mode, the polymer chains relax via the convective constraint release (CCR) mechanism.⁶⁰⁻⁶⁵ For the CCR mechanism, the tube constraints are renewed when neighboring chains are swept away by flow, which occurs on a time scale of the order of the inverse of the strain rate $\dot{\gamma}^{-1}$.^{56,62} For very high shear rates ($\dot{\gamma} > \tau_R^{-1}$), the chain stretch mechanism is believed to dominate as the polymer chains become distorted within their tubes, unable to relax fast enough by Rouse modes to maintain their Gaussian conformations.⁶⁶⁻⁷¹ For hole growth at $T = 101^\circ\text{C}$, the shear rates are $\sim 10^{-4} \text{ s}^{-1}$, which is in the intermediate to high shear rate regime compared with reptation rates τ_d^{-1} of 10^{-6} to 10^{-10} s^{-1} and Rouse rates τ_R^{-1} of 10^{-4} to 10^{-7} s^{-1} .⁴¹ It has been suggested that chain stretch is less important for shear flows with no rotation,^{66,69} which is the case for hole growth,⁴⁷ such that we would expect CCR to be the dominant relaxation mechanism. We have found that

the time constant τ_1 , representing the exponential decay of the transient behavior in hole growth, is in excellent agreement with the relaxation time expected for the CCR mechanism ($\sim\dot{\gamma}^{-1} = \tau/2$) with $\tau/\tau_1 = 2.2 \pm 1.4$.⁴¹ This finding suggests that the transient behavior observed as linear hole growth at short times is the result of chain disentanglement via the CCR mechanism before a constant, reduced, steady-state density of entanglements, and hence $\eta(\dot{\gamma})$, is reached.

Another surprising feature of the hole growth process is that the initial, transient behavior is well described by a single relaxation time τ_1 . Usually polymer dynamics are much more complex with a distribution of relaxation times required to describe the linear viscoelastic behavior.⁷² We believe that the transient behavior in the present hole growth experiments is simpler than ordinary linear viscoelastic behavior because there is only one dominant relaxation mechanism (CCR) with a single relaxation time ($\sim\dot{\gamma}^{-1}$) in the intermediate shear rate regime ($\tau_d^{-1} < \dot{\gamma} < \tau_R^{-1}$). This allows the hole growth dynamics to be well described by the simple spring and dashpot model shown in Figure 2.

Differential Pressure Experiment: Characteristic Growth Time for Very Thin Films

Hole growth measurements using the differential pressure experiment (DPE) complement those performed using optical microscopy by extending the range of temperatures and measurable film thicknesses to lower values allowing hole growth times to be determined for very thin films that have a reduced value of the glass-transition temperature.^{3,4,7} In the DPE, a piston is used to actively maintain a very small ($<10^{-4}$ atm) pressure difference across the freely-standing film, which causes air to flow through the holes present in the film. In the DPE, the position of the piston is measured as a function of time. Once holes have formed, the piston drifts continuously in one direction with a rate that increases with time corresponding to the growth of holes in the films. The piston position is fit to a functional form that contains several fitting parameters including the characteristic growth time of the holes τ , and a mean time t_0 and a width t_w that describe the onset of hole formation in terms of a Gaussian distribution of hole onset times.³⁹ Although the optical microscopy results showed that $R(t)$ is described by eq 5, the DPE fitting function is derived assuming only simple exponential growth, eq 1, in order

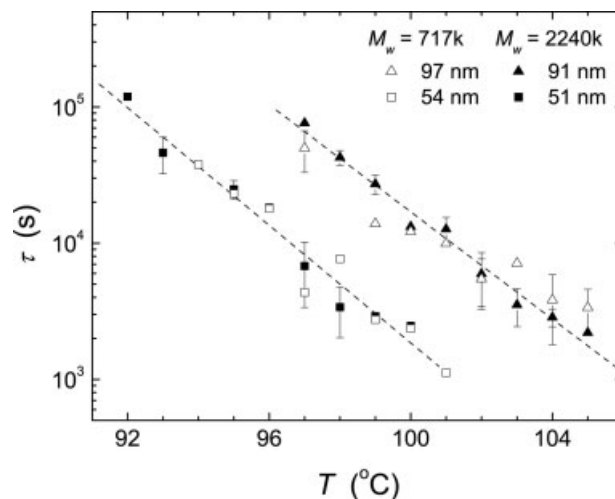


Figure 4. Characteristic growth time τ of the holes measured using the DPE plotted as a function of the measurement temperature T for freely-standing PS films of $M_w = 717 \times 10^3$ with $h = 97$ nm (Δ) and $h = 54$ nm (\square), and $M_w = 2240 \times 10^3$ with $h = 91$ nm (\blacktriangle) and $h = 51$ nm (\blacksquare). The dashed lines correspond to fits of the $\log_{10} \tau$ versus T data to a straight line for films with $M_w = 2240 \times 10^3$.

to simplify the data analysis. This assumption is justified since the DPE signal is dominated by gas flow through the largest holes in the film which are growing exponentially.^{39,40} For the range of temperatures that can be measured using both optical microscopy and the DPE, $101^\circ\text{C} < T < 105^\circ\text{C}$, we have demonstrated that the measured τ values are in agreement to within the reproducibility of the measurement with the τ values determined from optical microscopy measurements of $R(t)$ in late stage hole growth for which exponential growth is observed.⁴⁰

Figure 4 shows $\tau(T)$ values for a subset of the data collected using the DPE: film thicknesses $h = 97$ and 54 nm for $M_w = 717 \times 10^3$ and $h = 91$ and 51 nm for $M_w = 2240 \times 10^3$.⁴⁰ The set of films with the largest thicknesses have T_g values equal to the bulk value for PS, $T_g^{\text{bulk}} = 97^\circ\text{C}$, whereas the sets of films with smaller thicknesses have T_g values that are reduced from the bulk value ($T_g = 69^\circ\text{C}$ for $h = 54$ nm of $M_w = 717 \times 10^3$ and $T_g = 25^\circ\text{C}$ for $h = 51$ nm of $M_w = 2240 \times 10^3$).^{4,7} In Figure 4, it can be seen that the $\tau(T)$ curves for the thinnest films are shifted only slightly (4.7°C) to lower temperatures compared with the thickest films. It is clear that there is not a direct correspondence between the shifts in the $\tau(T)$ data sets and the reduced T_g values. In addition, it can be seen from the data shown in Figure 4 that the

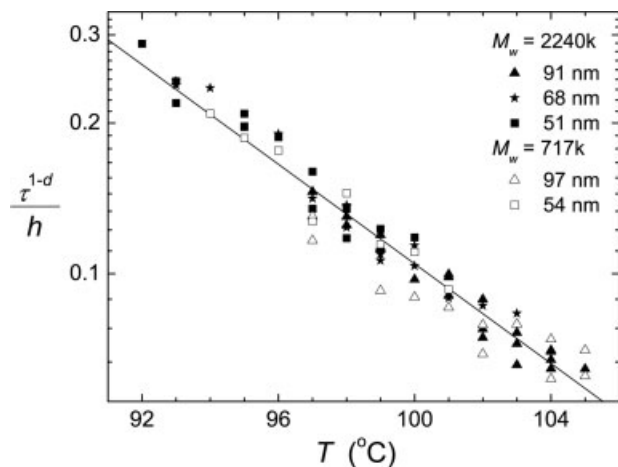


Figure 5. τ^{1-d}/h versus T , with $d = 0.77$, for all of the data collected with the DPE for freely-standing PS films of $M_w = 2240 \times 10^3$: $h = 91$ nm (\blacktriangle), $h = 68$ nm (\blackstar), and $h = 51$ nm (\blacksquare); and $M_w = 717 \times 10^3$: $h = 97$ nm (\triangle) and $h = 54$ nm (\square). The line is a best fit straight line to all of the data.

$\tau(T)$ values have no significant molecular weight dependence, which is consistent with nonlinear viscosity values $\eta(\dot{\gamma})$ that are reduced as a result of shear thinning.⁷³

The variations in $\tau(T)$ with film thickness h could possibly be related to changes in T_g with h for these films. However, before we can make this association, we must first account for the effects of the bulk phenomenon of shear thinning. The small shifts between the $\tau(T)$ data sets with thickness are consistent with an increase in shear thinning produced by the increase in stress acting at the edge of the holes as the film thickness is decreased ($\sigma = 2\epsilon/h$).⁴⁰ By combining eqs 2 and 3 with the empirical formula that describes shear thinning, which can be written as a power law decrease in viscosity η with increasing strain rate $\dot{\gamma}$ above a critical threshold $\dot{\gamma}_{cr}$.⁵⁰

$$\eta(\dot{\gamma}) = \eta_0 \left(\frac{\dot{\gamma}_{cr}}{\dot{\gamma}} \right)^d, \quad (11)$$

one can write

$$\frac{\tau^{1-d}}{h} = \frac{\eta_0 \dot{\gamma}_{cr}^d}{2^d \epsilon}. \quad (12)$$

By scaling the τ values according to eq 12, all of the $\tau(T)$ data collapse onto a single curve as shown in the plot of $(\tau^{1-d})/h$ vs. T in Figure 5. Note that $(\tau^{1-d})/h$ in eq 12 is independent of M_w , since the product $\eta_0 \dot{\gamma}_{cr}^d$, as specified by $\eta(\dot{\gamma})$ in eq 11 is independent of M_w in the shear thinning regime.⁷³

The DPE also provides a measure of the onset of hole formation. The DPE signal is fit by assuming a Gaussian distribution of hole onset times with a mean time t_0 and width t_w . In Figure 6 are shown the t_0 and t_w values plotted as a function of temperature for all of the films measured with the DPE. It can be seen that holes form more readily in the thinner films, but it should also be noted that holes form at temperatures comparable to T_{org}^{bulk} , even for the thinnest films that have a reduced value of $T_g = 25^\circ\text{C}$ ($h = 51$ nm of

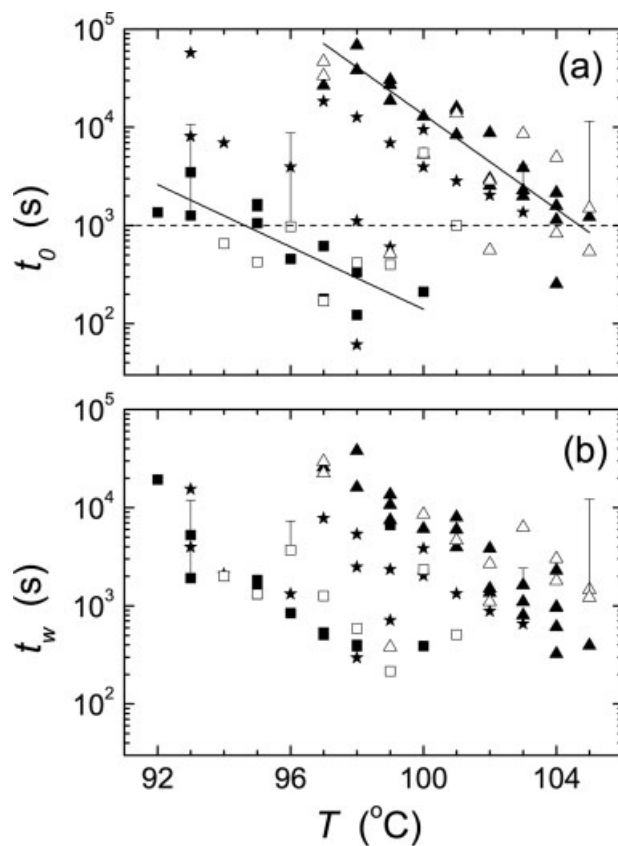


Figure 6. Best fit values of the (a) t_0 and (b) t_w parameters, which describe the Gaussian distribution of onset times, centered on time t_0 with width t_w used to model hole formation in the derivation of the DPE fitting function. Data are shown for all of the freely-standing PS films with $M_w = 2240 \times 10^3$: $h = 91$ nm (\blacktriangle), $h = 68$ nm (\blackstar), and $h = 51$ nm (\blacksquare); and $M_w = 717 \times 10^3$: $h = 97$ nm (\triangle) and $h = 54$ nm (\square). Representative error bars (positive-going only) are given for several data sets; each error bar represents the average of the uncertainties of the best fit values for that data set. In part (a), the solid lines correspond to best fit straight lines to the data for films with $M_w = 2240 \times 10^3$ and $h = 91$ nm (\blacktriangle), and $M_w = 2240 \times 10^3$ and $h = 51$ nm (\blacksquare), and the horizontal dashed line corresponds to an onset time of 1000 s.

$M_w = 2240 \times 10^3$). The onset time for hole formation at a given temperature is more likely shorter for the thinner films because the critical radius R_c for nucleation decreases with decreasing film thickness h , according to $R_c = h/2$.⁷⁴

DISCUSSION

As detailed in the Introduction section there have been numerous studies that have revealed dynamics in thin polymer films that differ from that in bulk. The reductions in T_g with decreasing film thickness suggest greatly enhanced segmental mobility in very thin films, while numerous studies of whole chain motion find that there is not a corresponding increase in mobility on this larger length scale (see ref. 12 for a recent review). How can we relate the results of these studies to those of the hole growth studies?

Hole growth measurements in freely-standing PS films have revealed complex flow processes: an initial, transient behavior as the system evolves into a steady-state behavior that is characterized by very large reductions in viscosity due to shear thinning, which is consistent with the relaxation times of the convective constraint release mechanism of the theory of entangled polymer dynamics. Both of these complex flow processes are produced by the large stress that acts at the edge of a growing hole in a very thin film, which leads to the decay of the initial set of physical entanglements between the molecules and the establishment of a state of high shear flow.

Because of the complexities of the surface-tension-driven fluid flow in very thin freely-standing PS films, it is challenging to relate the hole growth results to those obtained from measurements of the glass-transition temperature T_g and chain diffusion in thin polymer films, and corresponding computer simulations on confined polymers. For the purposes of this comparison, we focus instead on processes that occur during the formation of holes when the chains are still highly entangled, and the flow is driven by van der Waals forces acting across the film thickness (in the vicinity of a defect, e.g., dust).

Experimentally, we find that holes form only at temperatures comparable to or greater than the bulk value of T_g , even for films in which the T_g value is reduced by many tens of degrees with respect to the bulk value. To reconcile the T_g and hole formation results collected on similar freely-standing PS films, we consider three different

possibilities: there may be differences in mobility between directions parallel to and perpendicular to the plane of the film, there may exist variations in mobility across the thickness of the film particularly near a free surface, and segmental and whole chain motions may be effectively decoupled in thin films.

Evidence for reduced mobility perpendicular to the film plane and more mobility at the free surfaces than in the interior of thin polymer films could possibly explain why T_g values are reduced while holes form only at temperatures comparable to or greater than the bulk value of T_g in thin freely-standing PS films. For a hole to form in the film, sufficient chain mobility is required perpendicular to the film plane and across the entire thickness of the film. Therefore, if the mobility perpendicular to the film is reduced or if the chain segments at the center of the film move more slowly than the segments at the free surfaces of the film, then holes should not form until temperatures comparable to the bulk value of T_g are reached.

Differences in mobility parallel and perpendicular to the plane of the film have been observed in computer simulations in which it has been found that in-plane motions are enhanced while out-of-plane motions are reduced in thin films.⁷⁵⁻⁷⁹ Experiments involving the diffusion of labeled chains confined to thin supported films have measured slower dynamics than in the bulk in both the in-plane¹⁶ and out-of-plane²⁰⁻²² directions.

The presence of a more mobile surface layer has been proposed to explain T_g reductions in both supported and freely-standing PS films. This implies a gradient in the segmental mobility across the thickness of the film, and such a gradient has been observed directly using fluorescence measurements of supported multilayer films.^{13,80} In addition, single supported polymer films show a broadening of the glass transition with decreasing film thickness⁸¹⁻⁸⁶ that is consistent with either a variation in mobility across the film or a dynamical broadening of the distribution of relaxation times. In these measurements, it is the lower temperature portion of the transition that is shifted to even lower temperatures, while the high temperature onset of the transition remains at T_g^{bulk} such that the mid-point of the transition is observed to decrease with decreasing thickness.

It is problematic to interpret the freely-standing PS film results in terms of a gradient in mobility across the thickness of the films, since it is found experimentally that the glass transition

occurs over a narrow range of temperatures even for very thin films.^{3,5,7,10,12,87} One possible explanation for this sharp transition is that the segmental dynamics in freely-standing films is dominated by a single relaxation mechanism, such as the sliding motion proposed by de Gennes.^{88,89} The measurements of freely-standing films show reductions in T_g with decreasing film thickness of many tens of degrees Celsius such that very thin films may not have sufficient thickness to support such a large variation in mobility. This interpretation is suggested by recent fluorescence measurements on very thin supported multilayer films, which show that the dynamics across the thickness of the film become uniform, to within the precision of a single layer of the film (14 nm), for multilayer film thicknesses less than ~ 25 nm.¹³ The results of this analysis are puzzling, however, given that the reduced T_g results of low molecular weight freely-standing PS films, which exhibit a sharp glass transition suggestive of uniform segmental dynamics, are well described by a layer model that approximates the concept of a gradient in dynamics across the thickness of the film.^{5,6}

Based on a wide variety of experimental results, the basic idea of trying to infer the behavior of the mobility at one length scale from that at a different length scale in thin polymer films could be flawed. Some diffusion studies suggest that dynamics on longer length scales are reduced in thin polymer films,^{16,20–23,25} whereas the corresponding T_g values on similar or the same films are reduced. The combined T_g and hole formation results obtained for thin, freely-standing PS films discussed in the present manuscript also indicate that there can be a decoupling of the segmental and whole chain dynamics in very thin polymer films. Supporting evidence for this concept was obtained for supported PS films for which the thermal expansion of the glassy regime increased with decreasing film thickness, while that in the melt regime remained constant, resulting in a loss in contrast of the transition.⁸¹ These observations could be interpreted as a “freezing out” of slower modes on longer length scales at T_g^{bulk} , while the faster modes on shorter length scales persist to lower temperatures, resulting in a reduced value of T_g . Although the contrast between the glass and melt regions is also observed to decrease with decreasing thickness for freely-standing films, the changes in the slope of the melt and glass regions are less systematic than those observed for supported films.⁵

Collectively, these experimental results suggest that one should exercise caution in comparing the

results of measurements of the dynamics of thin polymer films on different length scales. To help understand the complicated dynamics of thin polymer films, measurements of relaxation time distributions as a function of film thickness and depth from the film surface are strongly encouraged.

CONCLUSIONS

Hole growth at low temperatures comparable to T_g^{bulk} shows complex viscoelastic behavior and pronounced shear thinning. Decreases in viscosity of over eight orders of magnitude have been measured with increasing strain rate. Careful measurements of the $R(t)$ behavior have allowed us to interpret the results in terms of a simple viscoelastic fluid model characterized by a characteristic growth time τ and a relaxation time τ_1 . The best fit τ and τ_1 values are consistent with ascribing the initial, transient behavior as that required to reach steady state flow because of the decay of entanglements via the CCR mechanism of the theory of entangled polymer dynamics. These results demonstrate that hole growth in freely-standing polymer films can be used as a microrheological probe to study nonlinear viscoelastic phenomena, and it is our hope that the data will allow quantitative tests of various constitutive equations and nonlinear viscoelastic theories.

Hole growth in very thin freely-standing films has been studied using a novel differential pressure experiment (DPE). Results from the DPE show that whole chain motion is not enhanced relative to that of the bulk, even for films in which large T_g reductions have been observed. It is our hope that these results will help to elucidate the complex nature of mobility on different length scales in thin freely-standing polymer films.

Financial support from the Natural Sciences and Engineering Research Council (NSERC) of Canada and the Province of Ontario (PREA program) is gratefully acknowledged.

REFERENCES AND NOTES

1. Keddie, J. L.; Jones, R. A. L.; Cory, R. A. *Europhys Lett* 1994, 27, 59.
2. Keddie, J. L.; Jones, R. A. L.; Cory, R. A. *Faraday Discuss* 1994, 98, 219.
3. Forrest, J. A.; Dalnoki-Veress, K.; Stevens, J. R.; Dutcher, J. R. *Phys Rev Lett* 1996, 77, 2002; *ibid.* 1996, 77, 4108.
4. Forrest, J. A.; Dalnoki-Veress, K.; Dutcher, J. R. *Phys Rev Lett* 1997, 56, 5705.

5. Mattsson, J.; Forrest, J. A.; Börjesson, L. *Phys Rev E* 2000, 62, 5187.
6. Forrest, J. A.; Mattsson, J. *Phys Rev E* 2000, 61, R53.
7. Dalnoki-Veress, K.; Forrest, J. A.; Murray, C.; Gigault, C.; Dutcher, J. R. *Phys Rev E* 2001, 63, 031801.
8. Roth, C. B.; Dutcher, J. R. *Eur Phys J E* 2003, 12, s01 024.
9. Forrest, J. A.; Jones, R. A. L. In *Polymer Surfaces, Interfaces and Thin Films*; Karim, A.; Kumar, S., Eds.; World Scientific: Singapore, 2000, p 251.
10. Forrest, J. A.; Dalnoki-Veress, K. *Adv Colloid Interface Sci* 2001, 94, 167.
11. Special Issue on Properties of Thin Polymer Films, *Eur Phys J E* 2002, 8, 99–266.
12. Roth, C. B.; Dutcher, J. R. In *Soft Materials: Structure and Dynamics*; Dutcher, J. R.; Marangoni, A. G., Eds.; Marcel Dekker: New York, 2004, p 1.
13. Ellison, C. J.; Torkelson, J. M. *Nature Mater* 2003, 2, 695.
14. Ellison, C. J.; Mundra, M. K.; Torkelson, J. M. *Macromolecules* 2005, 38, 1767.
15. Liem, H.; Cabanillas-Gonzalez, J.; Etchegoin, P.; Bradley, D. D. C. *J Phys: Condens Matter* 2004, 16, 721.
16. Frank, B.; Gast, A. P.; Russell, T. P.; Brown, H. R.; Hawker, C. *Macromolecules* 1996, 29, 6531.
17. Forrest, J. A.; Dalnoki-Veress, K. *J Polym Sci Part B: Polym Phys* 2001, 39, 2664.
18. Kawaguchi, D.; Tanaka, K.; Kajiyama, T.; Takahara, A.; Tasaki, S. *Macromolecules* 2003, 36, 1235.
19. Boiko, Y. M.; Prud'homme, R. E. *J Polym Sci Part B: Polym Phys* 1998, 36, 567.
20. Zheng, X.; Rafailovich, M. H.; Sokolov, J.; Strzemechny, Y.; Schwarz, S. A.; Sauer, B. B.; Rubinstein, M. *Phys Rev Lett* 1997, 79, 241.
21. Pu, Y.; Rafailovich, M. H.; Sokolov, J.; Gersappe, D.; Peterson, T.; Wu, W.-L.; Schwarz, S. A. *Phys Rev Lett* 2001, 87, 206101.
22. Pu, Y.; White, H.; Rafailovich, M. H.; Sokolov, J.; Patel, A.; White, C.; Wu, W.-L.; Zaitsev, V.; Schwarz, S. A. *Macromolecules* 2001, 34, 8518.
23. Kuhlmann, T.; Kraus, J.; Müller-Buschbaum, P.; Schubert, D. W.; Stamm, M. *J Non-Cryst Solids* 1998, 235–237, 457.
24. Hall, D. B.; Torkelson, J. M. *Macromolecules* 1998, 31, 8817.
25. Fakhraai, Z.; Valadkhan, S.; Forrest, J. A. *Eur Phys J E* 2005, 18, 143.
26. Reiter, G. *Macromolecules* 1994, 27, 3046.
27. Stange, T. G.; Evans, D. F.; Hendrickson, W. A. *Langmuir* 1997, 13, 4459.
28. Seemann, R.; Herminghaus, S.; Jacobs, K. *Phys Rev Lett* 2001, 87, 196101.
29. Masson, J.-L.; Green, P. F. *Phys Rev Lett* 2002, 88, 205504.
30. Masson, J.-L.; Green, P. F. *Phys Rev E* 2002, 65, 031806.
31. Reiter, G. *Phys Rev Lett* 2001, 87, 186101.
32. Reiter, G. *Eur Phys J E* 2002, 8, 251.
33. Reiter, G.; Sferrazza, M.; Damman, P. *Eur Phys J E* 2003, 12, 133.
34. Damman, P.; Baudelet, N.; Reiter, G. *Phys Rev Lett* 2003, 91, 216101.
35. Reiter, G.; Hamieh, M.; Damman, P.; Slavovs, S. E.; Gabriele, S.; Vilmin, T.; Raphaël, E. *Nature Mater* 2005, 4, 754.
36. Debrégeas, G.; Martin, P.; Brochard-Wyart, F. *Phys Rev Lett* 1995, 75, 3886.
37. Debrégeas, G.; de Gennes, P.-G.; Brochard-Wyart, F. *Science* 1998, 279, 1704.
38. Dalnoki-Veress, K.; Nickel, B. G.; Roth, C.; Dutcher, J. R. *Phys Rev E* 1999, 59, 2153.
39. Roth, C. B.; Nickel, B. G.; Dutcher, J. R.; Dalnoki-Veress, K. *Rev Sci Instrum* 2003, 74, 2796.
40. Roth, C. B.; Dutcher, J. R. *Phys Rev E* 2005, 72, 021803.
41. Roth, C. B.; Deh, B.; Nickel, B. G.; Dutcher, J. R. *Phys Rev E* 2005, 72, 021802.
42. Xavier, J. H.; Pu, Y.; Li, C.; Rafailovich, M. H.; Sokolov, J. *Macromolecules* 2004, 37, 1470.
43. Xavier, J. H.; Li, C.; Rafailovich, M. H.; Sokolov, J. *Langmuir* 2005, 21, 5069.
44. Brenner, M. P.; Gueyffier, D. *Phys Fluids* 1999, 11, 737.
45. Culick, F. E. C. *J Appl Phys* 1960, 31, 1128.
46. Ranz, W. E. *J Appl Phys* 1959, 30, 1950.
47. Roth, C. B. Ph.D. thesis, University of Guelph, Guelph, ON, Canada, August 2004.
48. Plazek, D. J.; O'Rourke, V. M. *J Polym Sci: Part A-2* 1971, 9, 209.
49. Ngai, K. L.; Plazek, D. J. In *Physical Properties of Polymers Handbook*; Mark, J. E., Ed.; AIP: Woodbury, NY, 1996; Ch. 25.
50. Graessley, W. W. *Adv Polymer Sci* 1974, 16, 1.
51. Schweizer, T. *J Rheol* 2003, 47, 1071.
52. Onogi, S.; Masuda, T.; Kitagawa, K. *Macromolecules* 1970, 3, 109.
53. Schausberger, A.; Schnindlauer, G.; Janeschitz-Kriegl, H. *Rheol Acta* 1986, 24, 1985.
54. O'Connell, P. A.; McKenna, G. B. *Science* 2005, 307, 1760.
55. Si, L.; Massa, M. V.; Dalnoki-Veress, K.; Brown, H. R.; Jones, R. A. L. *Phys Rev Lett* 2005, 94, 127801.
56. McLeish, T. C. B. *Adv Phys* 2002, 51, 1379.
57. Watanabe, H. *Prog Polym Sci* 1999, 24, 1253.
58. Leal, L. G.; Oberhauser, J. P. *Korea-Australia Rheol J* 2000, 12, 1.
59. Bent, J.; Hutchings, L. R.; Richards, R. W.; Gough, T.; Spares, R.; Coates, P. D.; Grillo, I.; Harlen, O. G.; Read, D. J.; Graham, R. S.; Likhtman, A. E.; Groves, D. J.; Nicholson, T. M.; McLeish, T. C. B. *Science* 2003, 301, 1691.
60. Marrucci, G. *J. Non-Newtonian Fluid Mech* 1996, 62, 279.
61. Ianniruberto, G.; Marrucci, G. *J. Non-Newtonian Fluid Mech* 1996, 65, 241.

62. Mead, D. W.; Larson, R. G.; Doi, M. *Macromolecules* 1998, 31, 7895.
63. Ianniruberto, G.; Marrucci, G. *Proc Int Congr Rheol* 2000, 2, 102.
64. Likhtman, A. E.; Milner, S. T.; McLeish, T. C. B. *Phys Rev Lett* 2000, 85, 4550.
65. Milner, S. T.; McLeish, T. C. B.; Likhtman, A. E. *J Rheol* 2001, 45, 539.
66. Marrucci, G.; Grizzuti, N. *Gazz Chim Ital* 1988, 118, 179.
67. Pearson, D.; Herbolzheimer, E.; Grizzuti, N.; Marrucci, G. *J Polym Sci Part B: Polym Phys* 1991, 29, 1589.
68. Mead, D. W.; Leal, L. G. *Rheol Acta* 1995, 34, 339.
69. Mead, D. W.; Yavich, D.; Leal, L. G. *Rheol Acta* 1995, 34, 360.
70. Mhetar, V.; Archer, L. A. *J. Non-Newtonian Fluid Mech* 1999, 81, 71.
71. Graham, R. S.; Likhtman, A. E., McLeish, T. C. B.; Milner, S. T. *J Rheol* 2003, 47, 1171.
72. Ward, I. M. *Mechanical Properties of Solid Polymers* 2nd ed.; Wiley: New York, 1983.
73. Stratton, R. A. *J. Colloid Interface Sci* 1966, 22, 517.
74. Gunton, J. D.; Miguel, M. S.; Sahni, P. S. In *Phase Transitions and Critical Phenomena*; Domb, C.; Lebowitz, J. L., Eds.; Academic Press: London, 1983; Vol. 8, p 267.
75. Baschnagel, J.; Binder, K. *J. Phys I France* 1996, 6, 1271.
76. Mansfield, K. F.; Theodorou, D. N. *Macromolecules* 1989, 22, 3143.
77. Bitsanis, I.; Hadziioannau, G. *J Chem Phys* 1990, 92, 3827.
78. Matsuda, T.; Smith, G. D.; Winkler, R. G.; Yoon, D. Y. *Macromolecules* 1995, 28, 165.
79. Doruker, P.; Mattice, W. L. *Macromolecules* 1999, 32, 194.
80. Priestley, R. D.; Ellison, C. J.; Broadbelt, L. J.; Torkelson, J. M. *Science* 2005, 309, 456.
81. Kawana, S.; Jones, R. A. L. *Phys Rev E* 2001, 63, 021501.
82. Hall, D. B.; Hooker, J. C.; Torkelson, J. M. *Macromolecules* 1997, 30, 667.
83. Hartmann, L.; Gorbatschow, W.; Hauwecte, J.; Kremer, F. *Eur Phys J E* 2002, 8, 145.
84. Fukao, K.; Miyamoto, Y. *Phys Rev E* 2000, 61, 1743.
85. Fukao, K.; Miyamoto, Y. *Europhys Lett* 1999, 46, 649.
86. Fukao, K.; Uno, S.; Miyamoto, Y.; Hoshino, A.; Miyaji, H. *Phys Rev E* 2001, 64, 051807.
87. Forrest, J. A. *Eur Phys J E* 2002, 8, 261.
88. de Gennes, P.-G. *Eur Phys J E* 2000, 2, 201.
89. de Gennes, P.-G. *C R Acad Sci Paris, Série IV* 2000, 1, 1179.